

Experimental Studies of Spiral-Confined HSCFST Columns under Uni-Axial Compression

Mianheng Lai, Johnny Ching Ming Ho, Hoat Joen Pam

Abstract—Concrete-filled-steel-tube (CFST) columns are becoming increasingly popular owing to the superior behavior contributed by the composite action. However, this composite action cannot be fully developed because of different dilation properties between steel tube and concrete. During initial compression, there will be de-bonding between the constitutive materials. As a result, the strength, initial stiffness and ductility of CFST columns reduce significantly. To resolve this problem, external confinement in the form of spirals is proposed to improve the interface bonding. In this paper, a total of 14CFST columns with high-strength as well as ultra-high-strength concrete in-filled were fabricated and tested under uni-axial compression. From the experimental results, it can be concluded that the proposed spirals can improve the strength, initial stiffness, ductility and the interface bonding condition of CFST columns by restraining the lateral expansion of steel tube and core concrete. Moreover, the failure modes of confined core concrete change due to the strong confinement provided by spirals.

Keywords—Concrete-filled-steel-tube, confinement, failure mode, high-strength concrete, spirals.

I. INTRODUCTION

THANKS to the rapid development of modern concrete technology, the production of high-strength concrete (HSC) or ultra-high-strength concrete (UHSC) with high workability is easily achievable [1]. However, previous research studies have revealed that this kind of concrete is more brittle than normal-strength concrete (NSC) [2], [3]. As a result, to confine such kind of concrete, a much higher transverse steel ratio should be provided if the same level of confinement as in the traditional reinforced-concrete (RC) columns is to be achieved. This may increase difficulty in the fabrication and more importantly, the concrete placing quality is hard to control, causing problems like honeycombing and segregation. Moreover, the confining pressure provided by the transverse reinforcement is very complex and highly non-uniform due to the arching action [4]. In consequence, the confinement effect could not be fully utilized. Therefore, in RC columns, HSC or UHSC is rarely adopted.

To further push up the strength limit of concrete in practical design and construction, concrete-filled-steel-tube (CFST) column is advocated. A CFST column, which consists of a hollow-steel-tube in-filled with concrete, exhibits better

performances than an RC column [5]-[7]. The placement of steel tube at the outer perimeter of the section is the most effective way of using material because the steel tube can provide the highest moment of inertia and thus the flexural capacity [5]. Besides, the inward buckling of steel tube is prevented by the core concrete, resulting in higher local buckling load [8], [9]. In return, the steel tube will provide large confining pressure and resist part of the compressive load simultaneously. This kind of confinement can change the stress state of core concrete into tri-axial state, which improves the strength, stiffness and ductility of the core concrete. Moreover, during construction, the steel tube can act as formwork such that no external formwork for concreting is needed, which can shorten the construction cycle time and save the labor as well as material cost. By adopting HSC or UHSC, higher strength-to-weight ratio can be achieved and the column size can be further reduced without jeopardizing the ductility. Thus, CFST columns are becoming more and more popular.

However, due to the different dilation properties of concrete and steel tube [10], [11], there will be de-bonding between the core concrete and steel tube at the initial stage of loading if the concrete and steel tube are loaded simultaneously under uni-axial compression. The de-bonding will reduce the confining pressure and thus the elastic strength, initial stiffness and ductility of the CFST columns. One of the consequences is the increase in the overall drift ratio of tall buildings, which may not fulfil the serviceability limit state requirement. Although the adverse effect by de-bonding can be neutralized when the expansion of concrete overcomes that of steel tube, the influences of de-bonding on the reduction of strength, initial stiffness and ductility cannot be ignored especially for thin-walled CFST columns in-filled with HSC. O'Shea and Bridge [12] reported that the lack of interface bonding would increase the chances of tube local buckling at elastic stage if thin-walled structural steel was adopted. Giakoumelis and Lam [13] concluded that bonding between steel tube and concrete would not affect the axial capacity for concrete strength smaller than 50 MPa. However, when the concrete strength exceeded 100 MPa, the bonded specimen would have axial capacity 14% larger than that of un-bonded specimen.

To fully utilize the confinement effect of CFST columns, the interface bonding condition must be improved. Previously, numerous researchers proposed different methods. For example, Huang et al. [14] adopted stiffened cross section; Cai and He [15] used binding bars; Hu et al. [16] proposed to confine CFST columns with FRP wraps. Besides, the authors conducted some experimental tests for improving the interface bonding of CFST columns using external confinements in the form of tie bars [17]

M. H. Lai is a PhD student of the Department of Civil Engineering, The University of Hong Kong, Hong Kong (phone: 852-2241-5390; fax: 852-2559-5337; e-mail: lmh58743@hku.hk).

J. C. M. Ho is a Senior Lecturer of the School of Civil Engineering, The University of Queensland, QLD 4072, Australia (e-mail: johnny.ho@uq.edu.au).

H.J. Pam is an Associate Professor of the Department of Civil Engineering, The University of Hong Kong, Hong Kong (e-mail: pamhoatjoen@hku.hk).

and rings [10]. All of these research studies showed that with additional restraint, the interface bonding condition can be enhanced and the strength, initial stiffness as well as ductility can be improved. In this study, the authors propose external steel, in the form of spirals welded on the external surface of CFST columns to restrain the lateral dilation of steel tube and core concrete. To verify the effectiveness of spirals, a total of 14 CFST columns were fabricated and tested under uni-axial load. All of these specimens were in-filled with concrete having cylinder strength from 104.5 to 125.3 MPa. The main parameters are: concrete cylinder strength (104.5, 125.3 MPa), confining scheme (spiral-confined, no confinement), spacing of spirals (45, 65, 80 mm) and lastly, diameter of spirals (6, 8 mm). From the experiment, it can be concluded that: (1) The core concrete of ultra-high-strength CFST (UHSCFST) columns could not maintain its integrity and two separate wedges were formed along the shear failure plane. Owing to the strong confinement provided by the spirals, core concrete of the spiral-confined UHSCFST columns could remain intact and the angle of rupture was significantly reduced. (2) Spirals were highly effective in improving the strength, initial stiffness and ductility of CFST columns. (3) Larger diameter and closer spacing of spirals could further improve the uni-axial behavior of high-strength CFST (HSCFST) columns.

II. EXPERIMENTAL PROGRAM

A. Test Specimens

A total of 14 HSCFST and UHSCFST columns were fabricated and tested under uni-axial load. The grade of steel

tube for both HSCFST and UHSCFST columns was S275 as per BS EN 10210-2:2006 [18]. The nominal diameter (D) and thickness (t) of the steel tube were respectively 139.7 mm and 4 mm. The measured values of D and t of the steel tube for all the specimens are listed in Table I. In order to reduce the end effects and minimize the slenderness effect of the specimens, it was recommended by previous research [19]-[21] that the height (H) of the columns should be three times the diameter. Thus, the steel tubes were fabricated to be 420 mm in height. The specimens were divided into two groups depending on the concrete cylinder strength: (1) 7 HSCFST columns with strength of 100 MPa; (2) 7 UHSCFST columns with strength of 120 MPa. In each group, one of the specimens was unconfined (without spiral), which served as control specimen. The rest of the specimens were confined by spirals with different diameters, d (6, 8 mm) and at different spacing, S ($45\text{ mm} \approx 10t$, $65\text{ mm} \approx 15t$, $80\text{ mm} \approx 20t$). The nominal and actual yield strengths of spirals were 250 and 304 MPa respectively. The spirals were intermittently welded to the external surface of the steel tube at four spots within one spacing of spirals. The welding spots were evenly distributed around the circumference of the steel tube, which were separated from each other by 90° . According to Chinese code [22], to fully develop the yield strength of the spirals, horizontal hoops with at least 1.5 times the circumference should be provided at both ends of spiral confinements. The horizontal hoops were also intermittently welded at four spots. Details of the specimens are shown in Fig. 1.

TABLE I
LISTS OF SPECIMENS

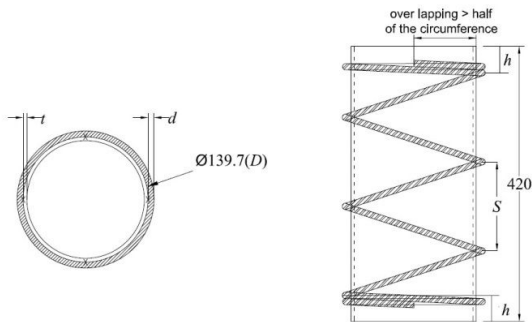
| Group No. | Specimens | σ_{cy} (MPa) | f_c (MPa) | Thickness of steel tube, t (mm) | Diameter of steel tube, D (mm) | Spacing of spirals, S (mm) | Diameter of spiral, d (mm) | Number of spiral, n |
|-----------|-------------------|---------------------|-------------|-----------------------------------|----------------------------------|------------------------------|------------------------------|-----------------------|
| 1 | CS(8)10-4-139-100 | 289.5 | 104.5 | 3.99 | 138.77 | 45 | 8 | 8 |
| | CS(6)10-4-139-100 | 289.5 | 104.5 | 4.00 | 139.22 | 45 | 6 | 8 |
| | CS(8)15-4-139-100 | 289.5 | 104.5 | 3.97 | 138.95 | 65 | 8 | 6 |
| | CS(6)15-4-139-100 | 289.5 | 104.5 | 3.98 | 138.99 | 65 | 6 | 6 |
| | CS(8)20-4-139-100 | 289.5 | 104.5 | 4.01 | 139.06 | 80 | 8 | 5 |
| | CS(6)20-4-139-100 | 289.5 | 104.5 | 3.96 | 139.13 | 80 | 6 | 5 |
| | CN0-4-139-100 | 289.5 | 104.5 | 4.00 | 138.69 | | Unconfined | |
| 2 | CS(8)10-4-139-120 | 289.5 | 125.3 | 3.97 | 139.35 | 45 | 8 | 8 |
| | CS(6)10-4-139-120 | 289.5 | 125.3 | 4.00 | 139.06 | 45 | 6 | 8 |
| | CS(8)15-4-139-120 | 289.5 | 125.3 | 4.01 | 138.98 | 65 | 8 | 6 |
| | CS(6)15-4-139-120 | 289.5 | 125.3 | 3.98 | 139.29 | 65 | 6 | 6 |
| | CS(8)20-4-139-120 | 289.5 | 125.3 | 3.98 | 139.11 | 80 | 8 | 5 |
| | CS(6)20-4-139-120 | 289.5 | 125.3 | 3.98 | 139.13 | 80 | 6 | 5 |
| | CN0-4-139-120 | 289.5 | 125.3 | 3.95 | 139.11 | | Unconfined | |

A naming system was established to identify the specimens. For example, CS(8)20-4-139-100 represents an HSCFST column (indicated by the first letter "C") confined by spirals (indicated by the second letter "S"), the diameter of spiral hoops is 8 mm (indicated by the number inside the parenthesis), the spacing of the spirals (See S in Fig. 1 (b)) is about 20 times the thickness of the steel tube (indicated by the first number after the parenthesis), the nominal thickness of the steel tube is 4 mm (indicated by the second number after the parenthesis), the

nominal diameter of the steel tube is about 139 mm (indicated by the third number after the parenthesis), and the concrete cylinder strength at the testing day is about 100 MPa (indicated by the last number, "100"). Specimen labelled with CN0-4-139-100 is the unconfined counterpart with CS(8)20-4-139-100, where N0 stands for "no confinement". Table I summarizes the material properties of all the HSCFST specimens.



(a) From left to right: N0, S(6)20, S(6)15, S(6)10, S(8)20, S(8)15 and S(8)10



(b) Spiral-confined CFST columns

Fig. 1 Typical test specimens

B. Instrumentation and Testing Procedure

In this experiment, similar to the authors' past research [10], the SATEC Series RD Model with maximum load of 5000 kN and maximum displacement of 100 mm was adopted. Details of the test set-up and instrumentation are shown in Fig. 2. Three linear variable differential transducers (LVDTs) with 100 mm measuring displacement were installed between the top and bottom loading platens to record the full length axial displacement of the CFST columns. Three bi-directional strain gauges (Tokyo Sokki Kenkyujo Co., Ltd, type: FCA-5-11-3L), separated by 120° each, were installed at around the mid-height of the external surface of the specimens to measure the longitudinal and lateral strains at the mid-height of steel tube.

All the specimens were tested under displacement control. For CFST columns, the top surface was levelled with a layer of rapid hardening gypsum before preloading was applied. After about 5 minutes of preloading, the specimens were unloaded and the test began. The initial loading rate was 0.3 mm / min for the first 10 mm. After that, the loading rate increased at a rate of 0.05 mm / min for every 1 mm increase in the axial displacement. The test was terminated when the displacement reached larger than 25 mm, which was about 0.06 strain; when the applied load dropped to less than 70% of the measured maximum load or when the applied load reached 4500 kN, which was 90% of the machine capacity, whichever was the earliest.

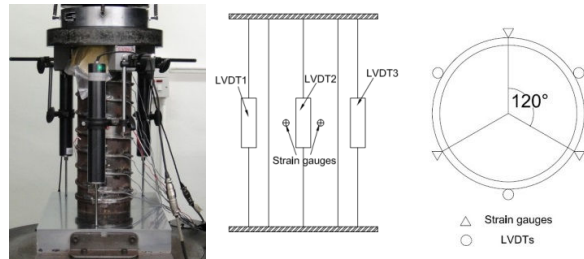


Fig. 2 Test set-up and instrumentation

III. EXPERIMENTAL RESULTS

The tested results of all the CFST columns are summarized below, which include failure modes of specimens and axial load against axial strain (displacement) curves.

A. Failure Modes

The failure mode for the CFST columns, whether spiral-confined or unconfined, due to the supporting effect provided by the core concrete, was outward folding. It can be seen from Figs. 3 (a) and (b) the failure mode of these specimens was irregular bulges between the spirals. For example, for specimen CS(6)20-4-139-100, two bulges were observed at different locations on the opposite sides, indicating shear failure plane between these two bulges.

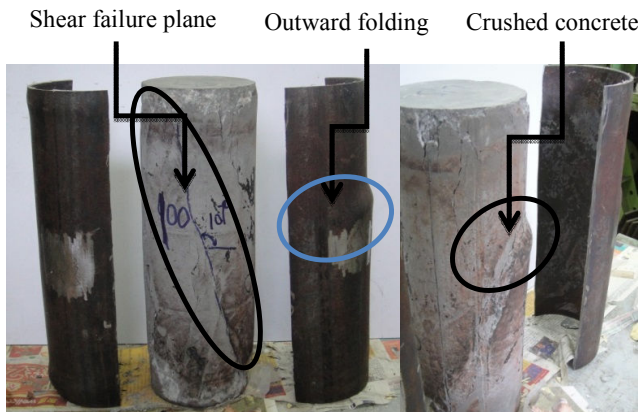
For a better visual image of the failure in the core concrete, the outer steel tube of some CFST columns was split and removed after the test. The exposed views of in-filled concrete of the unconfined CFST columns are given in Figs. 3 (c) and (d). It can be observed from Fig. 3 (c) that for HSCFST column filled with 100 MPa concrete, an obvious shear failure plane was formed and the measured angle of rupture was approximately 73° . Since the steel tube could offer some level of confinement to the core concrete, though not sufficient enough to avoid forming shear failure plane, the core concrete could maintain its integrity. For UHSCFST column with 120 MPa concrete in-filled (see Fig. 3 (d)), the steel tube could not effectively prevent the formation of shear sliding crack, resulting in two separated planes along the shear failure plane, and the angle of rupture for this specimen was also about 73° .



(a) Failure modes of confined HSCFST columns (100 MPa) From left to right: N0, S(6)20, S(6)15, S(6)10, S(8)20, S(8)15 and S(8)10



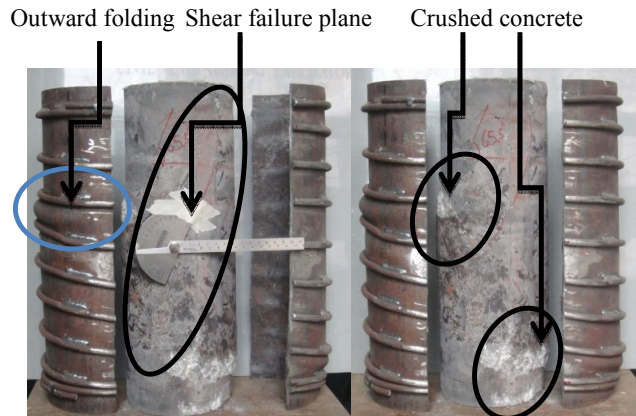
(b) Failure modes of confined UHSCFST columns (120 MPa) From left to right: N0, S(6)20, S(6)15, S(6)10, S(8)20, S(8)15 and S(8)10



(c) Failure modes of concrete core of HSCFST columns (CN0-4-139-100)



(d) Failure modes of concrete core of UHSCFST columns (CN0-4-139-120)



(e) Failure modes of concrete core of confined UHSCFST columns (CS(8)10-4-139-120)

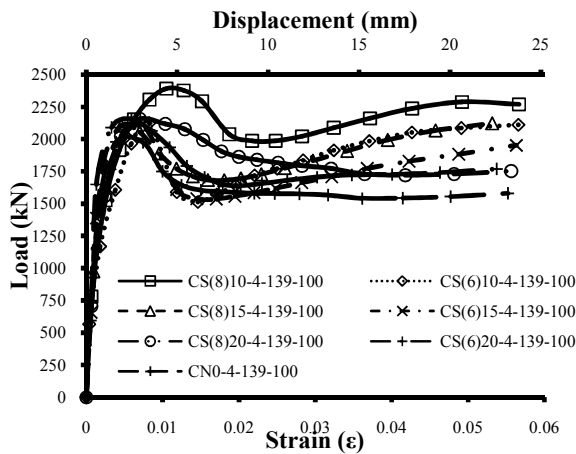
Fig. 3 Failure modes of HSCFST and UHSCFST columns

For specimen CS(8)10-4-139-120, which was filled with 120 MPa UHSC and confined by large diameter and close spacing spirals, it could be observed in Fig. 3 (e) that several bulges were found to be within the spacing of spirals. The locations of bulges were exactly the same with those of crushed concrete. This proved that the external spirals could provide effective confining pressure to the concrete core and hence reduce the effective length to within the spacing of spirals, where local buckling of steel tube would always occur. Compared with CN0-4-139-120, it was obvious that the core concrete of the spiral-confined specimen could remain its entirety and the angle of rupture was reduced to 65.5° . It can be concluded from the above analysis that the external spirals could provide strong confinement to the core concrete, thus leading to higher strength and ductility.

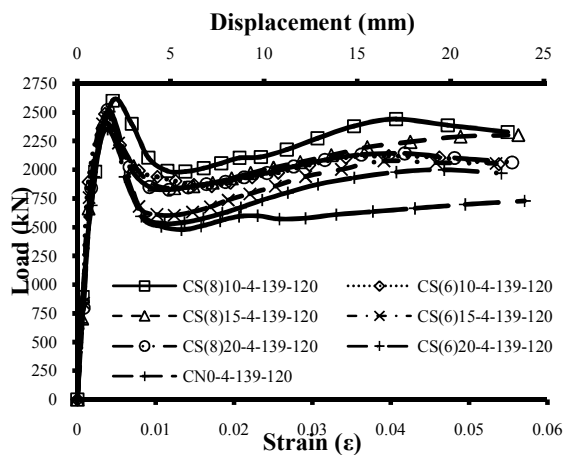
B. Axial Load against Axial Strain (Displacement) Curves

The axial stress is plotted against axial strain (displacement) for all the CFST columns in Fig. 4. It can be seen in Fig. 4 (a) for HSCFST columns (100 MPa) that initially the axial load increases linearly as the axial strain increases, and the slope for this linear portion is the initial stiffness of the columns, E_{cs} . As the axial strain increases further, there is a sudden drop indicating strength degradation during the post-elastic stage. This implies that the confinement provided by the steel tube and the spirals is not adequate to compensate the loss of strength due to the crushing of in-filled HSC. For UHSCFST columns in Group 2, it can be observed from Fig. 4 (b) that the load drops more rapidly than that in Group 1 after the peak strength, which is mainly attributed to the fact that UHSC is even more brittle than HSC and thus the strength degradation occurred at a faster rate. However, as the strain increases after the peak load, it can be noticed in Fig. 4 that the axial load-carrying capacity increases again for most of the specimens. This is because the lateral expansion of the core concrete increases significantly as the axial strain increases, pushing the steel tube locally and outward buckling of steel tube is formed at this stage, thus activating larger confining pressure and the axial load-carrying capacity of HSCFST as

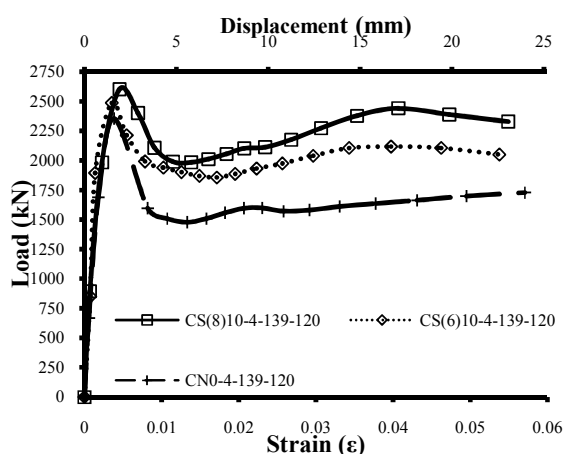
well as UHSCFST columns increases.



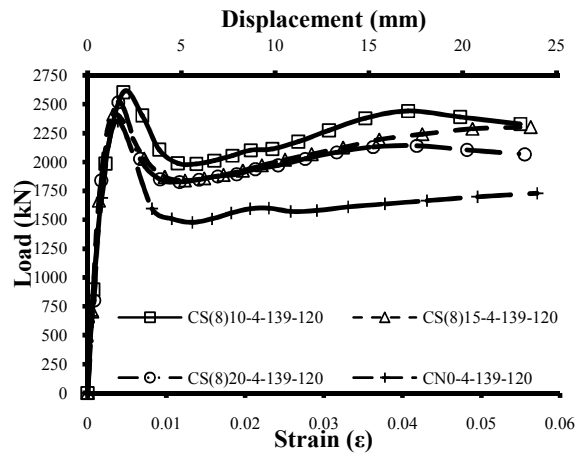
(a) Load-strain (displacement) curves for HSCFST columns (Group 1)



(b) Load-strain (displacement) curves for UHSCFST columns (Group 2)



(c) Load-strain (displacement) curves for UHSCFST columns (Different spiral diameter)



(d) Load-strain (displacement) curves for UHSCFST columns (Different spiral spacing)

Fig. 4 Load-strain (displacement) curves

Comparing different diameter of spirals, it is no doubt that confined UHSCFST columns with larger diameter of spirals exhibit larger strength and show more ductile behavior (see Fig. 4 (c)). With the same diameter of spirals, it can be observed from Fig. 4 (d) that specimens with smaller spacing of spirals behave better under uni-axial load. This is because with larger diameter and closer spacing of spirals, the confining pressure provided is stronger and more uniform, which enhances the strength, initial stiffness and ductility of HSCFST as well as UHSCFST columns.

To study the effectiveness of spirals, the ultimate experimental load N_{exp} , initial stiffness E_{cs} and strength degradation rate $\mu_{90\%}$ are reported in Table II. In this paper, N_{exp} is defined as the first peak strength. It can be seen from Table II that N_{exp} for spiral-confined specimens is larger than the unconfined counterpart. Moreover, with larger diameter or smaller spacing of spirals, N_{exp} is higher. The initial stiffness E_{cs} is calculated as the slope of initial straight portion of the axial load against axial strain curves and further divided by the total cross-section area of the columns, and all of the E_{cs} values are listed in Table II. From the table, it can be concluded that the initial stiffness for most of the spiral-confined specimens is larger than the unconfined one. In this paper, two parameters are selected to quantify the enhancements of strength and initial stiffness by adopting spirals, which were α and β respectively and they are defined as:

$$\alpha = \frac{N_{exp-c}}{N_{exp-u}} \quad (1)$$

$$\beta = \frac{E_{cs-c}}{E_{cs-u}} \quad (2)$$

where N_{exp-c} , N_{exp-u} are the ultimate experimental load for spiral-confined specimen and its unconfined counterpart

respectively; E_{cs-c} and E_{cs-u} are the initial stiffness for spiral-confined specimen and its unconfined counterpart respectively.

From Table II, it is evident that the strength and initial stiffness of spiral-confined specimens are larger than the respective unconfined one. For the strength, the average enhancement by adopting spirals as external confinement is 6.1%

and the maximum improvement is 16.0% for specimen CS(8)10-4-139-100. For the initial stiffness, the average increase is 5.8% and the maximum is 15.8%. From the above, it can be concluded that the external spirals are highly effective in improving the axial load and initial stiffness of HSCFST and UHSCFST columns.

TABLE II
STRENGTH, STIFFNESS AND STRAIN DEGRADATION RATE OF CFST COLUMNS

| Group No. | Specimens | E_{cs} (GPa) | Stiffness ratio, β | Ultimate strain, ϵ_{cu} | N_{exp} (kN) | Strength ratio, α | $\epsilon_{90\%}$ | $N_{90\%}$ (kN) | $\mu_{90\%}$ |
|-----------|-------------------|----------------|--------------------------|----------------------------------|----------------|--------------------------|-------------------|-----------------|--------------|
| 1 | CS(8)10-4-139-100 | 74.6 | 1.16 | 11082 | 2398 | 1.16 | 17275 | 2158 | 38.72 |
| | CS(6)10-4-139-100 | 71.6 | 1.11 | 8424 | 2128 | 1.03 | 10010 | 1915 | 134.17 |
| | CS(8)15-4-139-100 | 67.8 | 1.05 | 5150 | 2109 | 1.02 | 9372 | 1898 | 49.95 |
| | CS(6)15-4-139-100 | 70.2 | 1.09 | 5672 | 2086 | 1.01 | 10152 | 1877 | 46.56 |
| | CS(8)20-4-139-100 | 63.2 | 0.98 | 7809 | 2171 | 1.05 | 16206 | 1954 | 25.85 |
| | CS(6)20-4-139-100 | 72.9 | 1.13 | 5623 | 2161 | 1.04 | 10131 | 1945 | 47.94 |
| | CN0-4-139-100 | 64.3 | 1.00 | 5643 | 2070 | 1.00 | 8784 | 1863 | 65.90 |
| | CS(8)10-4-139-120 | 74.9 | 1.07 | 5101 | 2640 | 1.10 | 7125 | 2376 | 130.43 |
| 2 | CS(6)10-4-139-120 | 75.5 | 1.08 | 3854 | 2488 | 1.04 | 5354 | 2239 | 165.87 |
| | CS(8)15-4-139-120 | 74.3 | 1.06 | 4813 | 2566 | 1.07 | 5929 | 2309 | 229.93 |
| | CS(6)15-4-139-120 | 73.1 | 1.05 | 4002 | 2476 | 1.04 | 5277 | 2228 | 194.20 |
| | CS(8)20-4-139-120 | 64.9 | 0.93 | 4487 | 2577 | 1.08 | 5540 | 2319 | 244.73 |
| | CS(6)20-4-139-120 | 70.2 | 1.00 | 4600 | 2528 | 1.06 | 5245 | 2275 | 391.94 |
| | CN0-4-139-120 | 69.9 | 1.00 | 4204 | 2390 | 1.00 | 4752 | 2151 | 436.13 |

On the other hand, as mentioned by the authors' previous research [23], the strength degradation rate $\mu_{90\%}$ could act as an index for the deformability of the columns and is defined as:

$$\mu_{90\%} = -\frac{N_{exp} - N_{90\%}}{\epsilon_{exp} - \epsilon_{90\%}} \quad (3)$$

where $N_{90\%}$ is 90% strength of the ultimate experimental strength N_{exp} ; ϵ_{exp} and $\epsilon_{90\%}$ are strains corresponding to N_{exp} and $N_{90\%}$ respectively.

When $\mu_{90\%}$ is large, it means the immediate slope of post-peak portion is steep and thus the load drops rapidly, indicating brittle behavior of the specimen. The strain degradation rates $\mu_{90\%}$ for all the specimens are calculated and tabulated in Table II. $\mu_{90\%}$ for specimens CS(8)10-4-139-120, CS(8)10-4-139-120, CS(8)10-4-139-120 and CN0-4-139-120 are respectively 130.43, 229.93, 244.73 and 436.13, which means that $\mu_{90\%}$ increases as the spiral spacing increases. For most of the specimens, the larger the diameter of spirals, the smaller the $\mu_{90\%}$ is. This is because larger diameter and closer spacing of spirals can provide larger and more uniform confining pressure, thus improving the ductility of CFST columns. Comparing between the two concrete cylinder strengths, $\mu_{90\%}$ increases as the concrete cylinder strength increases. Moreover, for the specimen without any confinement and having higher concrete cylinder strength: CN0-4-139-120, $\mu_{90\%}$ is the largest (436.13) and obviously, this specimen presented the steepest slope in the post-peak region, as shown in Fig. 4 (b). This is because higher strength concrete will cause more brittle behavior and thus to maintain the same level of

ductility, larger confining pressure is needed.

IV. CONCLUSIONS

External spirals welded onto the exterior surface of steel tube is proposed in this study to restrict the lateral dilation of steel tube and the core concrete in order to improve the confining pressure and hence the interface bonding of CFST columns. To study the effectiveness of external spirals, a total of 14 specimens were fabricated and tested under uni-axial compression. From the tests, it is evident that:

- (1) The core concrete of UHSCFST columns cannot maintain its integrity and two separate wedges are formed along the shear failure plane with an angle of rupture equal to approximately 73°. Attributed to the strong confinement provided by the spirals, core concrete of the spiral-confined UHSCFST columns can remain intact and the angle of rupture is significantly reduced to 65.5°.
- (2) Spirals are highly effective in improving the ultimate strength of CFST columns by 6.1% on average and 16.0% on maximum. The axial load increases as the spacing of spirals decreases and diameter of spirals increases.
- (3) Spirals can effectively improve the initial stiffness of CFST columns (5.8% on average and 15.8% on maximum).
- (4) With spirals, the strength degradation rates of CFST columns reduce significantly. Larger diameter and closer spacing of spirals can further improve the ductility of CFST columns.

ACKNOWLEDGMENTS

The work described in this paper has been substantially supported by a grant from the Research Grants Council of the Hong Kong Special Administrative Region, China (Project No. HKU 712310E). Technical supports for the experimental tests provided by the laboratory staff of the Department of Civil Engineering, The University of Hong Kong, are gratefully acknowledged.

REFERENCES

- [1] A.K.H. Kwan, "Use of condensed silica fume for making high-strength, self-consolidating concrete," *Canadian Journal of Civil Engineering*, vol.27, no.4, pp. 620-627, 2000.
- [2] H.J. Pam, A.K.H. Kwan and M.S. Islam, "Flexural strength and ductility of reinforced normal-and high-strength concrete beams," *Proceedings of the Institution of Civil Engineers. Structures and Buildings*, vol.146, no.4, pp. 381-389, 2001.
- [3] J.C.M. Ho, A.K.H. Kwan and H.J. Pam, "Theoretical analysis of post-peak flexural behaviour of normal-and high-strength concrete beams," *The Structural Design of Tall and Special Buildings*, vol.12, no.2, pp. 109-125, 2003.
- [4] J.B. Mander, M.J.N. Priestley and R. Park, "Theoretical stress-strain model for confined concrete," *Journal of Structural Engineering*, vol.114, no.8, pp. 1804-1826, 1988.
- [5] L.H. Han, "Flexural behaviour of concrete-filled steel tubes," *Journal of Constructional Steel Research*, vol.60, no.2, pp. 313-337, 2004.
- [6] L.H. Han, S.H. He and F.Y. Liao, "Performance and calculations of concrete filled steel tubes (CFST) under axial tension," *Journal of Constructional Steel Research*, vol.67, no.11, pp. 1699-1709, 2011.
- [7] B. Uy, "Ductility, strength and stability of concrete-filled fabricated steel box columns for tall buildings," *The structural design of tall buildings*, vol.7, no.2, pp. 113-133, 1998.
- [8] M.A. Bradford, H.Y. Loh and B. Uy, "Slenderness limits for filled circular steel tubes," *Journal of Constructional Steel Research*, vol.58, no.2, pp. 243-252, 2002.
- [9] B. Uy, "Local and post-local buckling of concrete filled steel welded box columns," *Journal of Constructional Steel Research*, vol.47, no.1-2, pp. 47-72, 1998.
- [10] M.H. Lai and J.C.M. Ho, "Behaviour of uni-axially loaded concrete-filled-steel-tube columns confined by external rings," *The Structural Design of Tall and Special Buildings*, <http://dx.doi.org/10.1002/tal.1046>, 2012.
- [11] B. Persson, "Poisson's ratio of high-performance concrete," *Cement and concrete research*, vol.29, no.10, pp. 1647-1653, 1999.
- [12] M.D. O'Shea and R.Q. Bridge, "Design of circular thin-walled concrete filled steel tubes," *Journal of Structural Engineering*, vol.126, no.11, pp. 1295-1303, 2000.
- [13] G. Giakoumelis and D. Lam, "Axial capacity of circular concrete-filled tube columns," *Journal of Constructional Steel Research*, vol.60, no.7, pp. 1049-1068, 2004.
- [14] C.S. Huang, Y.K. Yeh, G.Y. Liu, H.T. Hu, K.C. Tsai, Y.T. Weng, S.H. Wang and M.H. Wu, "Axial load behavior of stiffened concrete-filled steel columns," *Journal of Structural Engineering*, vol.128, no.9, pp. 1222-1230, 2002.
- [15] J. Cai and Z.Q. He, "Axial load behavior of square CFT stub column with binding bars," *Journal of Constructional Steel Research*, vol.62, no.5, pp. 472-483, 2006.
- [16] Y.M. Hu, T. Yu and J.G. Teng, "FRP-confined circular concrete-filled thin steel tubes under axial compression," *Journal of Composites for Construction, ASCE*, vol.15, no.5, pp. 850-860, 2011.
- [17] J.C.M. Ho and M.H. Lai, "Behaviour of uni-axially loaded CFST columns confined by tie bars," *Journal of Constructional Steel Research*, vol.83, pp. 37-50, 2013.
- [18] BS EN 10210-2: *Hot finished structural hollow sections of non-alloy and fine grain steels. Tolerances, dimensions and sectional properties*, BSI, London, UK, 2006.
- [19] L.H. Han, G.H. Yao and X.L. Zhao, "Tests and calculations for hollow structural steel (HSS) stub columns filled with self-consolidating concrete (SCC)," *Journal of Constructional Steel Research*, vol.61, no.9, pp. 1241-1269, 2005.
- [20] J.P. Liu, S.M. Zhang, X.D. Zhang and L.H. Guo, "Behavior and strength of circular tube confined reinforced-concrete (CTRC) columns," *Journal of Constructional Steel Research*, vol.65, no.7, pp. 1447-1458, 2009.
- [21] Z.W. Yu, F.X. Ding and C.S. Cai, "Experimental behavior of circular concrete-filled steel tube stub columns," *Journal of Constructional Steel Research*, vol.63, no.2, pp. 165-174, 2007.
- [22] GB50010-2010: *Code for design of concrete structures*, Ministry of Housing and Urban-Rural Development of the People's Republic of China, Beijing, China, 2010 [In Chinese].
- [23] M.H. Lai and J.C.M. Ho, "Confinement effect of ring-confined concrete-filled-steel-tube columns under uni-axial load," *Engineering Structures* [Submitted].

Mr. Mianheng LAI is currently a PhD student at the Department of Civil Engineering, The University of Hong Kong. He obtained his Bachelor of Engineering degree from the same university with First Class Honor. His research interests are flexural strength, ductility and deformability of concrete-filled-steel-tube columns with and without confinements.

Ir. Dr. Johnny Ching Ming HO is Senior Lecturer of the School of Civil Engineering, The University of Queensland. Before joining the university in 2013, Dr Ho has worked as an Assistant Professor in The University of Hong Kong, and as a Civil Engineer in both Hong Kong and Brisbane offices of Arup on some large scale infrastructure projects such as The Stonecutters Bridge in Hong Kong and Ipswich Motorway Upgrade in Queensland, Australia. Dr Ho's research interests are ductility and deformability of high-strength concrete beams and columns, plastic hinge analysis of reinforced concrete members and behaviour of single- and double-skinned concrete-filled-steel-tube columns with external confinement and internal concrete expansive agent.

Ir. Dr. Hoatjoen PAM is an Associate Professor in the Department of Civil Engineering, The University of Hong Kong. She obtained her first degree in civil engineering from Parahyangan Catholic University, Indonesia. Subsequently, she obtained Master and PhD degrees in civil engineering from the University of Canterbury, New Zealand. She worked as a structural engineer in a consulting firm in New Zealand prior to joining The University of Hong Kong. Her research interests include strength and ductility of reinforced concrete members, and design of earthquake resistant structures.